Selective addressing of high-rank atomic polarization moments

V. V. Yashchuk,[1,*] D. Budker,[1,2] W. Gawlik,[3] D. F. Kimball,[1] Yu. P. Malakyan,[4] and S. M. Rochester[1]

[1]*Department of Physics, University of California at Berkeley, Berkeley, California 94720-7300*
[2]*Nuclear Science Division, Lawrence Berkeley National Laboratory, Berkeley, California 94720*
[3]*Instytut Fizyki im. M. Smoluchowskiego, Uniwersytet Jagielloński, Reymonta 4, 30-059 Krakow, Poland*
[4]*Institute for Physical Research, National Academy of Sciences of Armenia, Ashtarak-2, 378410, Armenia*

(Dated: February 22, 2003)

We describe a method of selective generation and study of polarization moments of up to the highest rank $\kappa = 2F$ possible for a quantum state with total angular momentum F. The technique is based on nonlinear magneto-optical rotation with frequency-modulated light. Various polarization moments are distinguished by the periodicity of light-polarization rotation induced by the atoms during Larmor precession and exhibit distinct light-intensity and frequency dependences. We apply the method to study polarization moments of ^{87}Rb atoms contained in a vapor cell with antirelaxation coating. Distinct ultra-narrow (1-Hz wide) resonances, corresponding to different multipoles, appear in the magnetic-field dependence of the optical rotation. The use of the highest-multipole resonances has important applications in quantum and nonlinear optics and in magnetometry.

PACS numbers: PACS 32.80.Bx,32.80.-t,95.75.Hi

High-rank polarization moments (PM) and associated high-order coherences have recently drawn attention (see [1, 2, 3, 4, 5, 6, 7, 8] and references therein) because they may enhance nonlinear optical effects important in applications such as electromagnetically induced transparency [9], creation of nonclassical atomic and photonic states [10], realization of photon blockades [11], quantum gates [12], photonic switches [13], and atomic magnetometry [14, 15].

While signatures of high-order PM were detected in several experiments [3, 4, 5, 6, 8], the methods used in these investigations are not sufficiently selective and/or do not allow real-time manipulation of particular multipoles. Here we describe a method, based on nonlinear optical rotation with frequency-modulated light (FM NMOR) [16], by which one can selectively induce, control, and study any possible multipole moment. Applying the method to ^{87}Rb atoms in a paraffin-coated cell [17, 18], we have verified the expected power and spectral dependences of the resonant signals and obtained a quantitative comparison of relaxation rates for the even-rank moments.

The density matrix in the M, M' representation for a state with total angular momentum F can be decomposed into PM of rank $\kappa = 0 \ldots 2F$, uncoupled under rotations, with components $q = -\kappa \ldots \kappa$:

$$\rho_q^{(\kappa)} = \sum_{M,M'=-F}^{F} (-1)^{F-M'} \langle F, M, F, -M' | \kappa, q \rangle \rho_{M,M'},$$

where $\langle \ldots | \ldots \rangle$ indicate the Clebsch-Gordan coefficients (see, for example, [19]). For a given choice of quantization axis, $|q| \neq 0$ components of the PM are related to coherences between Zeeman sublevels for which $\Delta M = M - M' = q$, while $q = 0$ components depend on sublevel populations. Thus, coherences $\rho_{M,M'}$ contribute to all PM with $\kappa \geq |\Delta M|$ and a $|\Delta M| = 2F$ coherence is uniquely associated with the highest PM for a given state, e.g., the quadrupole moment ($\kappa = 2$) for $F = 1$, or the hexadecapole ($\kappa = 4$) for $F = 2$. The method introduced here exploits the different axial symmetries of the PM (2-fold and 4-fold for the quadrupole and hexadecapole, respectively; Fig. 1) to selectively create and detect them (see also [3, 4, 5, 6]).

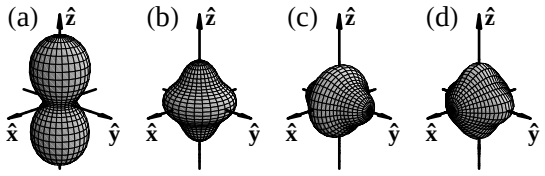

FIG. 1: Polarization moments visualized as discussed in [20] with surfaces for which the distance to the origin in a given direction is proportional to the probability of finding the projection $M = F$ along this direction. (a): "pure" quadrupole $\kappa = 2, q = 0$; (b): $\kappa = 4, q = 0$ hexadecapole; (c): same as in (b), but rotated by $\pi/2$ around the x-axis; (d): the average of (b) and (c), which has a 4-fold symmetry with respect to rotations around $\hat{\mathbf{x}}$. In all cases, the minimum necessary amount of $\rho_0^{(0)}$ was added to ensure that all sublevel populations are non-negative [20]. Probability surfaces (a) and (d) rotating around $\hat{\mathbf{x}}$-directed magnetic field with the Larmor frequency correspond to the polarization states produced in this experiment.

While multipole moments of rank $\kappa \leq 2$ can be easily generated and detected with weak light (since a photon has spin one), higher-rank moments require multi-photon interactions for both production *and detection*. In the present method, we use a single laser beam (which is still of sub-mW power) for the nonlinear interactions required to pump and probe the high-multipole moments.

Under conditions of our experiment, FM NMOR (Fig. 2) can be understood as a three-stage (pump, pre-

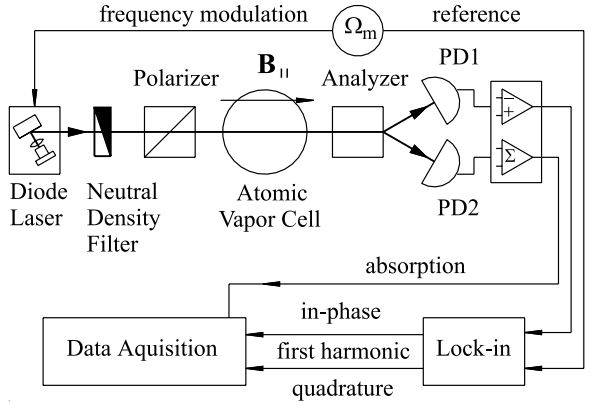

FIG. 2: Simplified diagram of the FM NMOR setup. The balanced polarimeter incorporating the analyzer and photodiodes PD1 and PD2 detects signals due to time-dependent optical rotation of linearly polarized frequency-modulated light.

cession, probe) process: atoms are polarized in an interaction with the laser beam (whose diameter is much smaller than the vapor cell dimensions), then leave the beam and bounce around the cell while undergoing Larmor precession, and finally return into the laser beam region and undergo the "probe" interaction. The laser light is frequency modulated, causing the optical pumping and probing to acquire a periodic time dependence. When the pumping rate is synchronized with the precession of atomic polarization, a resonance occurs and the atomic medium is pumped into a polarized state which rotates around the direction of the magnetic field at the Larmor frequency Ω_L. The optical properties of the medium are modulated at the frequency $\kappa\Omega_L$, due to the symmetry of atomic polarization with rank κ. For example, for the quadrupole moment the modulation is at $2\Omega_L$, and for the hexadecapole it is at $4\Omega_L$ [Fig. 1(a,d)]. This periodic change of the optical properties of the atomic vapor modulates the angle of the light polarization, leading to the FM NMOR resonances. If the time-dependent optical rotation is measured at the first harmonic of Ω_m, a resonance is seen when Ω_m coincides with $\kappa\Omega_L$ (Fig. 3) [25].

At the resonance for a PM of rank κ (which should be absent for states with $2F \leq \kappa$) we expect the signal amplitude to go as the κ-th power of light intensity at low intensities, as discussed below. Next, we show that these predictions are verified in this experiment.

In the present experiment (Fig. 2), we used the FM NMOR technique [16] with ^{87}Rb atoms. The central laser frequency was tuned near various hfs components of the D1 line. The typical light power was a few hundred μW and the laser beam diameter was $\sim$3 mm. The laser frequency was modulated at $\Omega_m/(2\pi)$ from 50 Hz to 1 kHz, and the frequency modulation amplitude was approximately 40 MHz (peak-to-peak). The vapor cell, with isotopically enriched ^{87}Rb, is 10 cm in diameter and has an

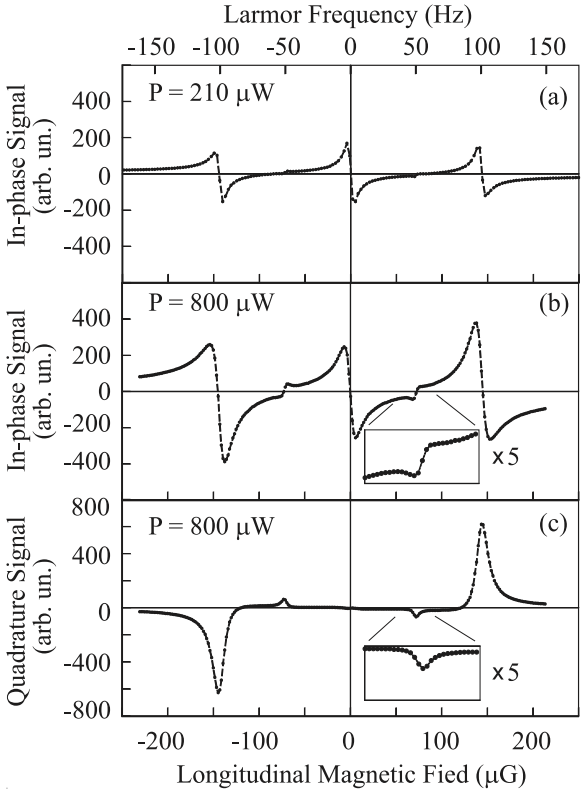

FIG. 3: An example of the magnetic-field dependence of the FM NMOR signals showing quadrupole resonances at $B = \pm 143.0$ μG, and the hexadecapole resonances at ± 71.5 μG. Laser modulation frequency is 200 Hz, modulation amplitude is 40 MHz peak-to-peak; the central frequency is tuned to the low-frequency slope of the $F = 2 \rightarrow F' = 1$ absorption line. Plots (a,b) show the in-phase component of the signal at two different light powers; plot (c) shows the quadrature component. Note the increase in the relative size of the hexadecapole signals at the higher power. The insets show zooms on hexadecapole resonances.

antirelaxation coating and no buffer gas. The cell is surrounded with four layers of magnetic shielding. A system of coils inside the innermost shield is used to compensate the residual fields (at a level $\lesssim 0.1$ μG) and first-order gradients, and to apply a well-controlled, arbitrarily directed magnetic field to the atoms. This allows observation of FM NMOR resonances with magnetic-field widths of about 1 μG in the low-light-intensity limit.

Figure 3 shows the magnetic-field dependence of the observed FM NMOR signals. The central laser frequency was tuned to the low-frequency slope of the $F = 2 \rightarrow F' = 1$ absorption line as shown in Fig. 4. At relatively low light power [Fig. 3(a)], there are three prominent resonances: one at $B = 0$, and two corresponding to $2\Omega_L = \Omega_m$. Much smaller signals, whose relative amplitudes rapidly grow with light power, are seen at $4\Omega_L = \Omega_m$, the expected positions of the hexadecapole resonances.

The spectral dependences for both types of resonance

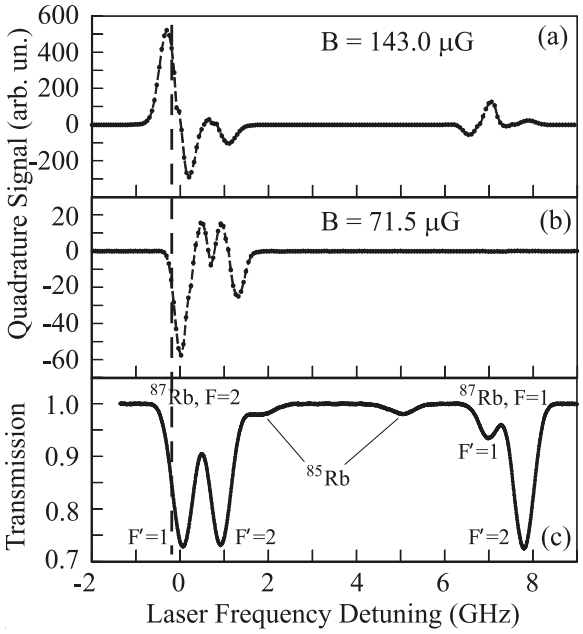

FIG. 4: Spectral dependences of the quadrupole (a) and the hexadecapole (b) signals measured at light power of 800 μW, and the low-power (.4 μW) transmission spectrum (no FM) (c). Note the different spectral dependences for the FM NMOR signals in (a) and (b), and in particular, the absence of the signal at the $F = 1 \rightarrow F'$ transitions in (b). The vertical line indicates the central laser frequency where the measurements represented in Figs. 3, 5, and 6 were taken.

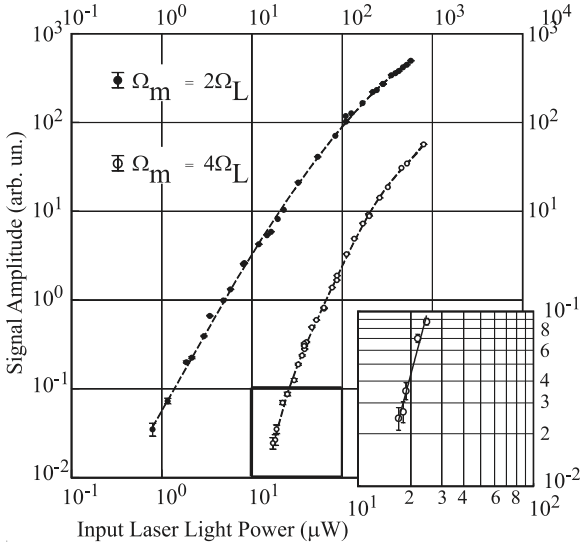

FIG. 5: Signal amplitude vs. the input laser power. Filled circles: the quadrupole resonance; open circles: the hexadecapole resonance. The inset shows the expanded low-power region for the latter. From these data, we determine the initial linear slope on these log-log plots (corresponding to the exponent in the power dependence of the signal) as 1.96(6) and 3.75(37) for the quadrupole and hexadecapole cases, respectively. The corresponding expected exponents are 2 and 4.

signals with fixed magnetic field and modulation frequency are shown in Fig. 4. While the quadrupole resonance signals [$\Omega_m = 2\Omega_L$; Fig. 4(a)] are observed for both ground-state hyperfine components, no signals are observed for the hexadecapole resonances [$\Omega_m = 4\Omega_L$; Fig. 4(b)] near the lines involving the $F = 1$ ground state, which can not support a hexadecapole moment [26]. The different shapes of the quadrupole and hexadecapole spectra near the $F = 2$ transition group require further analysis.

Light-intensity dependences of the resonance amplitudes are shown in Fig. 5. The observed low-intensity (I) asymptotics of these curves (which show saturation at higher intensities) scale approximately as I^2 and I^4. These power dependences and many other salient features of the observed resonances can be understood with the help of a simple model of an $F = 2 \rightarrow F' = 1$ transition with independent pumping, evolution in a magnetic field, and probing, in which to lowest-order, the quadrupole and hexadecapole moments are first ($\rho^{(2)} \propto I_{pump}$) and second order ($\rho^{(4)} \propto I_{pump}^2$) in light intensity, respectively. The component of the signal due to the induced optical rotation in the probe beam proportional to the quadrupole moment goes as $I_{probe}\rho^{(2)}$, while that proportional to the hexadecapole moment goes as $I_{probe}^2\rho^{(4)}$. The intensity dependences predicted by this model, as well as the periodicity of the signals with respect to Larmor precession and the relative widths of the resonances, match the observations from the experiment, in which a single beam serves as pump and probe.

Figure 6 shows the dependence of the resonance widths on power at a fixed magnetic field. While both the quadrupole and hexadecapole resonances exhibit power broadening, it is much less pronounced in the latter case. This is important for applications such as magnetometry because it allows operation at higher light powers with better statistical sensitivity [21]. In the zero-power limit, we find that the resonance widths (Fig. 6) for the two types of resonances tend to values near 1 μG with ratio $\Delta B_q/\Delta B_h = 0.94(4)$. The expected ratio of these widths is twice the ratio of the light-independent relaxation rates for the PM with $\kappa = 2$ and 4 [27]. Thus, we find that the light-independent relaxation rate for the hexadecapole is approximately twice that of the quadrupole. Relaxation of the PM in our experimental conditions is dominated by the residual relaxation on the paraffin-coated cell walls and spin-exchange collisions between Rb atoms. The electron-randomization collision model (see, for example, [22]), predicts that the quadrupole moment relaxes at a rate 3/8 that of the hexadecapole moment, which relaxes at the electron-randomization rate. Thus, the observed ratio of the widths is close to the expected.

In conclusion, we have developed and applied a new technique for the study of high atomic-polarization mo-

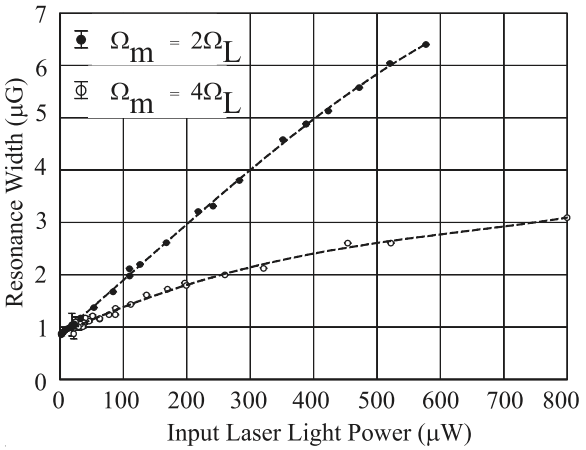

FIG. 6: Resonance width vs. the input laser power. Filled circles: the quadrupole resonance; open circles: the hexadecapole resonance. The widths extrapolated to zero light power are found to be $\Delta B_q = 0.848(4)$ μG and $\Delta B_h = 0.904(33)$ μG for the quadrupole and hexadecapole cases, respectively.

ments, allowing their selective creation and detection via corresponding well-resolved resonances. The study of the highest-rank PM signals in FM NMOR is important for the applications of this technique in Earth-field magnetometry [16]. This is because energy separation for Zeeman sublevels with $\Delta M = 2F$ of the $F = I + 1/2$ states of the alkali atoms is linear in the magnetic field, while separations between other sublevels are generally nonlinear due to magnetic-field mixing of states of different F. Therefore, it is advantageous to use of the FM NMOR resonances due to the $\Delta M = 2F$ coherence, as will be discussed in detail elsewhere.

Future work will explore the extension of the technique to separated pump and probe light beams and application to higher angular-momentum states. This will allow further optimization of the selective control of multipole moments and will elucidate the exact mechanisms responsible for the nonlinear light-atom interactions involved at the pump and the probe stages. Specifically, we will explore the role of conversion of the high-rank moments into alignment and orientation under the combined action of the magnetic field and the light shifts, which can be of crucial importance in nonlinear optical rotation [7, 20, 23, 24].

We thank M. Zolotorev for useful discussions and A. Vaynberg for crafting parts of the apparatus. This work has been supported by the Office of Naval Research (grant N00014-97-1-0214); by NRC US-Poland Twinning grant 015369, and by the Polish Committee for Scientific Research (grant PBZ/KBN/043/PO3/2001) and the National Laboratory of AMO Physics in Toruń, Poland; by a US-Armenian bilateral Grant CRDF AP2-3213/NFSAT PH 071-02; by NSF; and by the Director, Office of Science, Nuclear Science Division, of the U.S. Department of Energy under contract DE-AC03-76SF00098. D.B. also acknowledges the support of the Miller Institute for Basic Research in Science.

* Electronic address: yashchuk@socrates.berkeley.edu

[1] B. Łobodziński and W. Gawlik, Phys. Rev. A **54**(3), 2238 (1996).
[2] B. Łobodziński and W. Gawlik, Phys. Scr. **T70**, 138 (1997).
[3] D. Suter, T. Marty, and H. Klepel, Opt. Lett. **18**(7), 531 (1993).
[4] D. Suter and T. Marty, J. Opt. Soc. Am. B **11**(1), 242 (1994).
[5] J. D. Xu, G. Wäckerle, and M. Mehring, Phys. Rev. A **55**(1), 206 (1997).
[6] J. D. Xu, G. Wäckerle, and M. Mehring, Z. Phys. D **42**(1), 5 (1997).
[7] D. Budker, W. Gawlik, D. F. Kimball, S. M. Rochester, V. V. Yashchuk, and A. Weis, Rev. Mod. Phys. **74**(4), 1153 (2002).
[8] A. B. Matsko, I. Novikova, G. R. Welch, and M. S. Zubairy, Opt. Lett. **28**(2), 96 (2003).
[9] S. E. Harris, Phys. Today **50**(7), 36 (1997).
[10] A. S. Parkins, P. Marte, P. Zoller, and H. J. Kimble, Phys. Rev. Lett. **71**(19), 3095 (1993).
[11] A. Imamoglu, H. Schmidt, G. Woods, and M. Deutsch, Phys. Rev. Lett. **79**(8), 1467 (1997).
[12] Q. A. Turchette, C. J. Hood, W. Lange, H. Mabuchi, and H. J. Kimble, Phys. Rev. Lett. **75**(25), 4710 (1995).
[13] S. E. Harris and Y. Yamamoto, Phys. Rev. Lett. **81**(17), 3611 (1998).
[14] E. B. Alexandrov, A. S. Pazgalev, and J. L. Rasson, Opt. Spectrosk. **82**(1), 14 (1997).
[15] A. I. Okunevich, Opt. Spectrosk. **91**(2), 193 (2001).
[16] D. Budker, D. F. Kimball, V. V. Yashchuk, and M. Zolotorev, Phys. Rev. A **65**, 055403 (2002).
[17] E. B. Alexandrov, M. V. Balabas, A. S. Pasgalev, A. K. Vershovskii, and N. N. Yakobson, Laser Physics **6**(2), 244 (1996).
[18] E. B. Alexandrov, M. V. Balabas, D. Budker, D. S. English, D. F. Kimball, C. H. Li, and V. Yashchuk, Phys. Rev. A **66**(4) (2002).
[19] D. A. Varshalovich, A. N. Moskalev, and V. K. Khersonskii, *Quantum theory of angular momentum: irreducible tensors, spherical harmonics, vector coupling coefficients, 3nj symbols* (World Scientific, Singapore, 1988).
[20] S. M. Rochester and D. Budker, Am. J. Phys. **69**(4), 450 (2001).
[21] D. Budker, D. F. Kimball, S. M. Rochester, V. V. Yashchuk, and M. Zolotorev, Phys. Rev. A **62**(4), 043403/1 (2000).
[22] R. J. Knize, Z. Wu, and W. Happer, Advances in Atomic and Molecular Physics **24**, 223 (1988).
[23] D. Budker, D. F. Kimball, S. M. Rochester, and V. V. Yashchuk, Phys. Rev. Lett. **85**(10), 2088 (2000).
[24] S. M. Rochester, D. S. Hsiung, D. Budker, R. Y. Chiao, D. F. Kimball, and V. V. Yashchuk, Phys. Rev. A **63**(4), 043814/1 (2001).
[25] Additional resonances can be observed at higher harmonics [16].
[26] The spectral dependences shown in Fig. 4(a,b) were

obtained by subtracting the average of spectra of the quadrature component taken approximately 15 μG above and below the resonance from the spectrum recorded with magnetic field set at the resonance value. This procedure renders a measurement free from the small residual contribution from the zero-field resonance arising from the "transit" effect [16].

[27] It can be shown that the width of an FM NMOR resonance corresponding to a PM of rank κ goes as $\gamma_\kappa/(\kappa g\mu)$, where γ_κ is the rate of light-independent relaxation for a PM of rank κ, g is the gyromagnetic ratio, and μ is the Bohr magneton.